

RESEARCH ARTICLE

Delayed Wound Healing in Heat Stable Antigen (*HSA/CD24*)-Deficient Mice

Shiran Shapira^{1,5}, Oded Ben-Amotz^{1,3}, Osnat Sher², Dina Kazanov¹, Jacob Mashiah⁴, Sarah Kraus^{1,5}, Eyal Gur³, Nadir Arber^{1,4*}

1 The Integrated Cancer Prevention Center, Tel Aviv Sourasky Medical Center, Tel Aviv, Israel, **2** Unit of Bone and Soft Tissue Oncology, The Institute of Pathology, Tel Aviv Sourasky Medical Center, Tel Aviv, Israel, **3** Department of Plastic and Reconstructive Surgery, Tel Aviv Sourasky Medical Center, Tel Aviv, Israel, **4** Department of Dermatology, Tel Aviv Sourasky Medical Center, Tel Aviv, Israel, **5** Sackler Faculty of Medicine, Tel Aviv University, Tel Aviv, Israel

* narber@post.tau.ac.il



Abstract

Background

Healthy individuals rarely have problems with wound healing. Most skin lesions heal rapidly and efficiently within one to two weeks. However, many medical and surgical complications can be attributed to deficiencies in wound repair. Open wounds have lost the barrier that protects tissues from bacterial invasion and allows the escape of vital fluids. Without expeditious healing, infections become more frequent. The *CD24* gene encodes a heavily-glycosylated cell surface protein anchored to the membrane by phosphatidylinositol. *CD24* plays an important role in the adaptive immune response and controls an important genetic checkpoint for homeostasis and autoimmune diseases in both mice and humans. We have previously shown that overexpression of *CD24* results in increased proliferation and migration rates.

Aim

To examine the role of *CD24* in the wound healing process.

Methods

An excisional model of wound healing was used and delayed wound healing was studied in genetically modified heat stable antigen (*HSA/CD24*)-deficient mice (*HSA*^{-/-}) compared to wild-type (WT) mice.

Results

Large full-thickness skin wounds, excised on the back of mice, exhibited a significant delay in the formation of granulation tissue, and in wound closure when compared to their *WTHSA*^{+/+} littermates. Wounds were histologically analyzed and scored, based on the degree of cellular invasion, granulation tissue formation, vascularity, and re-epithelialization. Additionally, in stitched wounds, the *HSA*^{-/-} mice failed to maintain their stitches; they

OPEN ACCESS

Citation: Shapira S, Ben-Amotz O, Sher O, Kazanov D, Mashiah J, Kraus S, et al. (2015) Delayed Wound Healing in Heat Stable Antigen (*HSA/CD24*)-Deficient Mice. PLoS ONE 10(10): e0139787. doi:10.1371/journal.pone.0139787

Editor: Ajay Goel, Baylor University Medical Center, UNITED STATES

Received: June 16, 2015

Accepted: September 17, 2015

Published: October 6, 2015

Copyright: © 2015 Shapira et al. This is an open access article distributed under the terms of the [Creative Commons Attribution License](https://creativecommons.org/licenses/by/4.0/), which permits unrestricted use, distribution, and reproduction in any medium, provided the original author and source are credited.

Data Availability Statement: All relevant data are within the paper.

Funding: The authors have no support or funding to report.

Competing Interests: The authors have declared that no competing interests exist.

did not hold and fell already 24 hours, revealing erythematous wound fields. Re-expression of *HSA*, delivered by lentivirus, restored the normal healing phenotype, within 24 hours post-injury, and even improved the healing in WT, and in BalbC mice.

Conclusions

Delayed wound-healing in the absence of *HSA/CD24* suggests that *CD24* plays an important role in this process. Increased expression of *CD24*, even in the normal state, may be used to enhance wound repair.

Introduction

Most skin lesions heal rapidly and efficiently within one to two weeks [1]. Although being healed, the outcome is neither esthetically nor functionally perfect [2]. In the U.S. alone, 35 million cutaneous wounds require major intervention annually [2].

Normal wound healing is a complex, dynamic and fragile process that is impacted by many factors and is divided into three phases, inflammatory, proliferative and maturation or remodeling [3,4]. After an initial wound, a fibrin clot is formed. In the inflammatory phase, debris and bacteria undergo phagocytosis and removal. Cytokines are released to initiate the proliferative phase. This process manifests with chemotaxis, phagocytosis, angiogenesis, epithelization, collagen degradation and remodeling, production of new glycosaminoglycans and wound contraction. Wound healing is a highly regulated interplay between systematic expressed cell types (i.e., neutrophils, macrophages, fibroblasts, keratinocytes, endothelial cells), extracellular matrix insoluble components and a group of soluble mediators (i.e., growth factors, cytokines, chemokines) [2,3,5].

The healing process begins with an accumulation of neutrophils and monocytes in the damaged tissue to form a first line of defense. Thereafter, macrophages and mast cells emigrate from nearby tissues and the circulation and accumulate in order to initiate the specific immune response. These inflammatory cells are recruited to the wound site by specific chemotactic factors or chemokines [6,7]. Re-epithelialization and granulation tissue formation include migration of cells from the wound edge to fill the wound site. It involves the migration of keratinocytes over the impermanent matrix in order to rebuild a protective layer [8].

Rapid changes in the extracellular matrix (ECM) occur during the healing process. The fibrin clot is replaced by fibronectin and hyaluronan and subsequently by type I and III collagen [1]. The contribution of each component to the wound repair process is difficult to assess due to the complexity of cells involved in the healing.

The *CD24* gene encodes a heavily glycosylated cell surface protein anchored to the membrane by phosphatidylinositol⁶. Human *CD24* consists of 31 amino acids with 16 potential O-glycosylation and N-glycosylation sites. Owing to this extensive glycosylation, *CD24* has mucin-like characteristics [9]. It plays a crucial role in cell selection and maturation during hematopoiesis and is expressed mainly on premature lymphocytes and certain epithelial and neural cells [10,11]. *CD24* can function as an alternative ligand for P-selectin, an adhesion receptor on activated endothelial cells and platelets [12–14].

CD24 has been previously shown to play an important role in the inflammation [15] process. We also showed that overexpression of *CD24* increased proliferation, and migration rates *in vitro* [16–18].

Herein, it is shown that CD24 plays a major role in wound healing, in *HSA*^{-/-} knockout (KO) mice as well as normal mice. We explored our theory that CD24(HSA) may be involved and contribute to the healing process. We examined whether there is a relationship between the mice genotype, HSA expression, and the healing process and rate. We confirmed our observations by immunohistochemistry (IHC) and collagen staining, and most importantly by re-expression of the *HSA* gene. We suggest here, for the first time, a new candidate for improving and accelerating the healing process.

Materials and Methods

Animal housing and procedures

Heat stable antigens (*HSA*) knockout (KO) mice on a C57BL/6J background were kindly provided by Prof. Peter Altevogt (DKFZ Heidelberg, Germany). Wild-type (WT)*HSA*^{+/+} mice were purchased from Harlan Laboratories (Rehovot, Israel). All mice were fed with a standard pellet diet and had access to tap water *ad libitum*. The animals were maintained at a constant temperature (22±2°C) on a 12 h light/dark cycle and all procedures were approved by the Institutional Committee for Animal Welfare at Tel-Aviv Sourasky Medical Center. Before the procedures, mice were anesthetized by intraperitoneal (i.p.) injection of ketamine (50 mg/kg) and xylazine (5 mg/kg). The dorsal surface of the animal was cleaned, shaved, and sterilized with a betadine solution. Longitudinal incisions, 1.5–4 cm, were made on the back of the mice. The excised wounds were left open, stitched, or dressed with gauze after virus administration. In *HSA*/mCherry expression experiments, the virus-containing medium or antibodies were applied once post-wounding. Wound healing was examined by macroscopic observations and histological analysis every day after wound excision. At the end of the experiments, the animals were sacrificed with a lethal dose of CO₂.

Virus production

Three HIV-based viral vectors (kindly provided by Prof. Eran Bacharach, Tel Aviv University, Israel); pVSV-G (5 µg), pCMV.ΔR8.2 (15 µg) and pHR'CMV-*HSA* (or pHR'CMV-mCherry, as negative control) (20 µg) were co-transfected to HEK293T helper cells using the standard calcium phosphate transfection method. hours after transfection, virions-containing supernatants were collected, the pH was adjusted with Hepes, filtered and stored at -80°C.

Infection

Before the infection, polybrene was added to the virions-containing supernatant to a final concentration of 8µg/ml. The supernatant was added to NIH-3T3 cells, that were seeded in 6-cm plates the day before (5×10⁵ cells), for 2 hours. Then, 3 ml of fresh medium was added to the plate and after two days the infected cells were analyzed for the expression of the relevant gene.

In vivo, under anesthesia [intraperitoneal injection of ketamine (50 mg/kg) and xylazine (5 mg/kg)], 300 µl of viruses-containing medium were injected into the cells on the wound border or dropped directly into the wounds area of the mice. Wound closure and mice's well-being were monitored on a daily basis.

In vivo targeting of *HSA* by anti-*HSA* mAb

Before the procedures, mice were anesthetized [ketamine (50 mg/kg) and xylazine (5 mg/kg)]. Longitudinal incisions, of 2 cm, were made on the back of the mice. Ten mg/kg of Rat anti-mouse M1/69 IgG2b mAb was administrated topically by injection into the cells on the wound border. Wound closure and mice's well-being were monitored every day.

Imaging of mCherry expression in mice

For all imaging, mice were anesthetized using aketamine-xylazine mixture. For imaging of mCherry expression, mCherry-encoded viruses (300 μ l of viruses-containing medium) were injected into the cells on the wound border or dropped directly into the wounds area of WT mice immediately after injury. The mCherry expression was monitored 96 hours later using the Maestro *in vivo* fluorescence imaging of whole small animals' device.

Histology

At days 0, 3 and 14 days post-wounding, the animals were sacrificed with a lethal dose of CO₂, autopsied, and their wound beds surrounded by a margin of non-wounded skin were collected. Samples were fixed with 4% paraformaldehyde overnight at room temperature, embedded in paraffin blocks, and sectioned. After deparaffinization and rehydration, the sections were washed and stained with Hematoxylin and Eosin (H&E) or NovaUltra™ Picro-Sirius Red stain for collagen staining. Tissue sections were then washed, mounted, and visualized on an Olympus AH light microscope at 400 \times magnification.

Protein extraction and immunoblotting

For protein extraction, cells were washed with PBS, scraped and lysed in 1% Triton buffer (100 mM NaCl, 5 mM EDTA, 1% Triton, 50 mM Tris-HCl pH 7.5, 50 mM NaF, and a protease inhibitor cocktail (Roche), added just before use. Following 30 min of incubation on ice, lysates were cleared by centrifugation at 14,000 rpm for 10 min, at 4°C. For immunoblotting, protein samples were electrophoresed alongside a molecular weight marker on 10% SDS-Polyacrylamide gel electrophoresis (PAGE) and Western blot analysis was performed as described below.

Western Blot analysis

Proteins resolved by SDS-PAGE were electro-transferred onto the nitrocellulose membrane. The membrane was blocked for at least 1 h with PBST containing 5% skim milk at room temperature (RT) with slow agitation. Proteins were detected using a specific primary antibody (M1.69, generous gift from Prof. Peter Altevogt; DKFZ Heidelberg, Germany) followed by horseradish peroxidase (HRP)-conjugated secondary antibody and enhanced chemiluminescence (ECL) detection using the EZ-ECL reagent as described by the vendor (Biological Industries, Beith HaEmek).

Flow cytometry analysis

Cellular CD24 binding by rat M1.69 was evaluated by flow cytometry (FACS). Approximately 1×10^6 cells were used in each experiment. After trypsinization, the cells were washed in fluorescence-activated cell sorting (FACS) buffer (10% FBS, 0.01% sodium azide in ice-cold PBS) and fixed with 2% formaldehyde for 15 min at RT. After washing with FACS buffer, 100 μ l of 15 μ g/ml anti-CD24 were added for 30 min at RT. After washing X3 with FACS buffer, fluorescein isothiocyanate (FITC)-labeled goat anti-rat (1:100) was added for 30 min at RT. Detection of bound antibodies was performed on a FACSCalibur (Becton Dickinson, San Jose, CA) and results were analyzed with the CELLQuest program (Becton Dickinson).

Statistics

Data from the *in vivo* studies are presented as mean \pm SD of sets of data as determined for each group of mice. Statistical significant differences between groups and at different time points were determined by Student t-test, P values <0.05 were considered significant.

Wound areas were calculated by using the ImageJ software. Area selection was created and analyses for the areas were automatically done.

Results

Delayed wound healing in *HSA* KO mice

Several independent experiments with 10-mm oblong full-thickness excision wounds, including the striated muscle layer, on the dorsal skin of WT (*HSA*^{+/+}) (n = 5) and KO (*HSA*^{-/-}) (n = 5) mice demonstrated that the absence of HSA hampered the healing of skin wounds (Fig 1). Moreover, the KO mice failed to keep the stitches in the stitched wounds. Healing of KO mice wounds remained incomplete. In the *HSA* KO mice, scabs were thicker and erythematous wound fields were shown. Similar results were seen with longer excision wounds (n = 6) (Fig 2).

Histologic scoring [19] was based on the degree of cellular infiltration, granulation tissue formation, and re-epithelialization (Table 1). Wounds of WT mice had higher average histologic scores compared to the KO mice. There was a greater degree of cellular infiltration and capillary ingrowth in the *HSA*^{+/+} mice (Fig 3). In addition, the collagen scoring [20] (Table 2) confirmed the IHC staining; the fibers were still separated with complete loss of architecture in the *HSA*^{-/-} mice 72h after the wound was established (Fig 4).

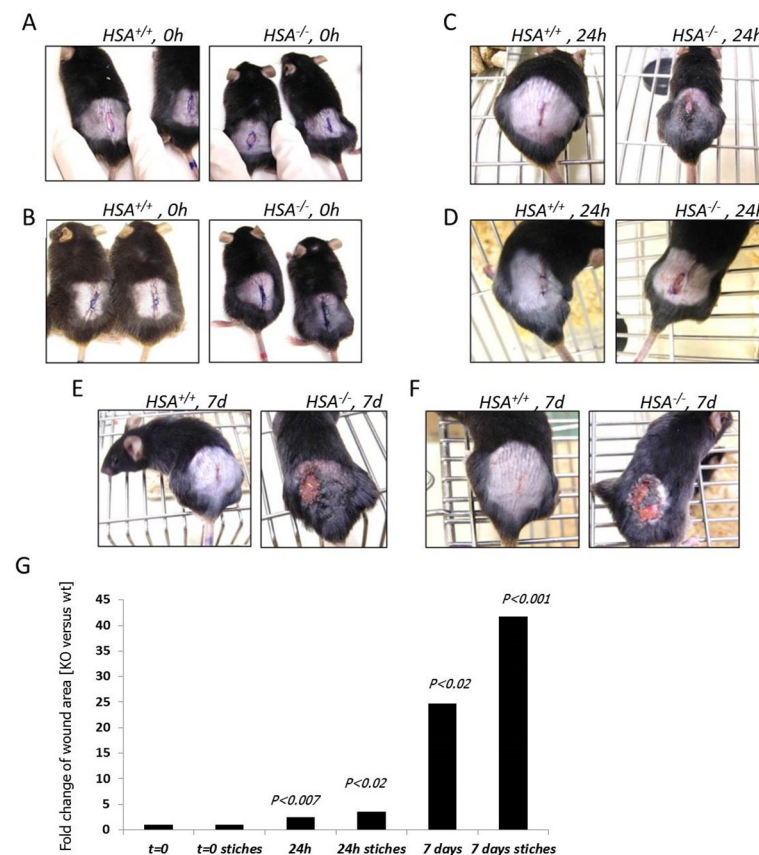


Fig 1. Wound closure of full-thickness wounds is delayed in *HSA*^{-/-} mice. The left picture in each panel represents the *HSA*^{+/+} mouse while the right is for the *HSA*^{-/-}. A. t = 0, time of injury. B. t = 0, the wounds were stitched upon injury. C. t = 24 h. D. t = 24 h, with stitches. E. t = 7 days. F. t = 7 days, with stitches. G. A representative plot of the statistical differences between the groups. Each bar shows the fold change of the wound area compared to t = 0.

doi:10.1371/journal.pone.0139787.g001

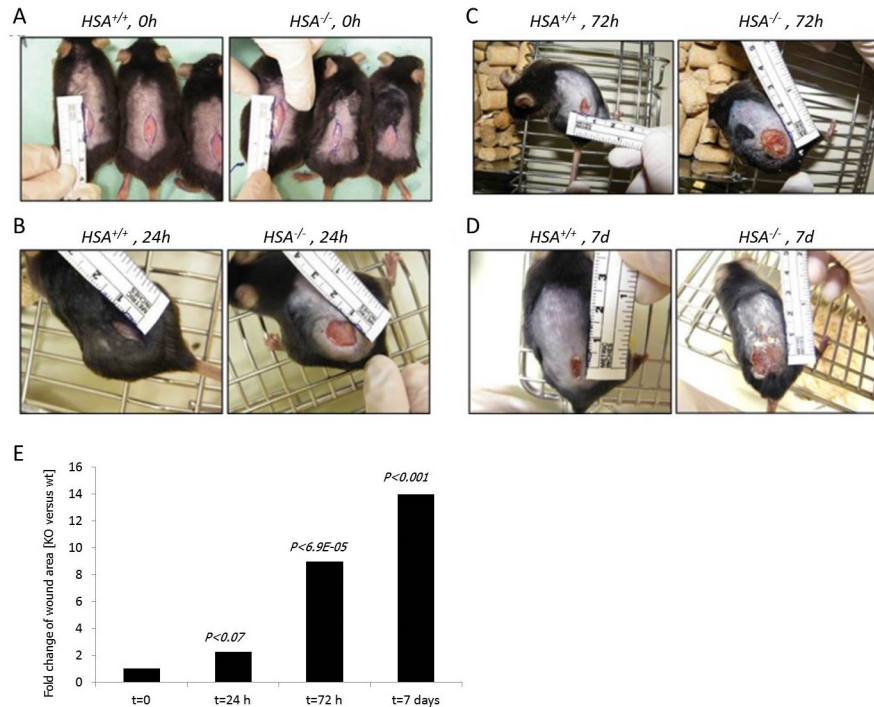


Fig 2. Wound closure of bigger full-thickness wounds is faster in *HSA*^{+/+} mice. The left picture in each panel represents the *HSA*^{+/+} mouse while the right is for the *HSA*^{-/-}. A. t = 0, time of injury. B. t = 24 h. C. t = 72 h. D. t = 7 days. E. A representative plot of the statistical differences between the groups. Each bar shows the fold change of the wound area compared to t = 0.

doi:10.1371/journal.pone.0139787.g002

Production of *HSA*-encoding viruses

Three viral-based vectors were used to deliver and express the *HSA* gene in the wounded tissue. First, the expression of the transgene by the helper cells, *in vitro*, was confirmed by monitoring the mCherry fluorescence marker (Fig 5A) and Western blot analysis (Fig 5C). Next, the infectivity of the produced virions was tested *in vitro* on NIH-3T3 cells. Seventy two hours post-infection of NIH-3T3 cells, the expression of the HSA/mCherry proteins was examined and confirmed by fluorescence microscopy (Fig 5B), Western blot (Fig 5C) and FACS analysis (Fig 5D).

Table 1.

1–3	None to minimal cell accumulation. No granulation tissue or epithelial travel					
4–6	Thin, immature granulation that is dominated by inflammatory cells but has few fibroblasts, capillaries or collagen deposition. Minimal epithelial migration					
7–9	Moderately thick granulation tissue, can range from being dominated by inflammatory cells to more fibroblasts and collagen deposition. Extensive neovascularization. Epithelium can range from minimal to moderate migration					
10–12	Thick, vascular granulation tissue dominated by fibroblasts and extensive collagen deposition. Epithelium partially to completely covering the wound					
	wt			KO		
t = 0	t = 72h	t = 14 days	t = 0	t = 72h	t = 14 days	
12	4–6	11–12	12	1–3	4–6	

doi:10.1371/journal.pone.0139787.t001

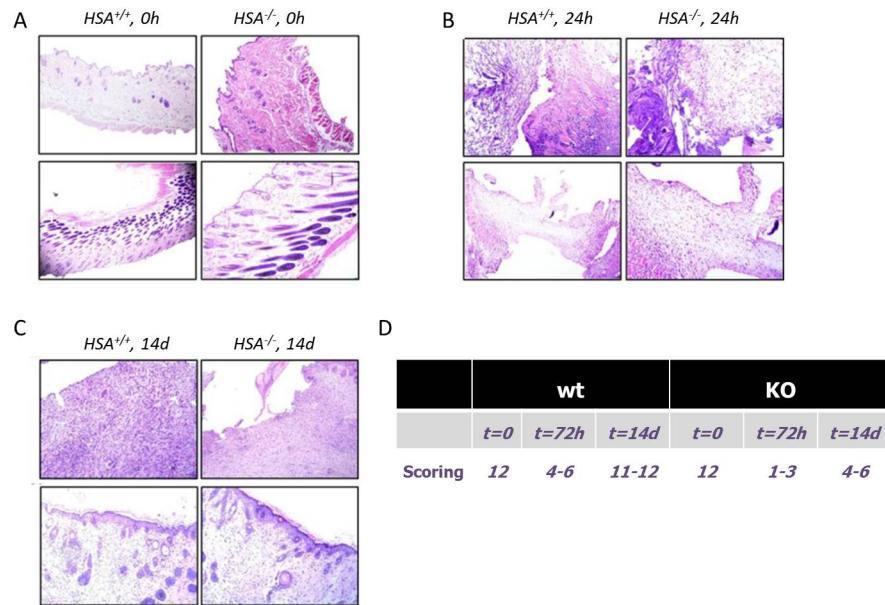


Fig 3. Histological stains. Tissue sections were stained with Hematoxylin and Eosin (H&E) and visualized on an Olympus AH light microscope at 400× magnification. The left picture in each panel represents the *HSA*^{+/+} mice while the right is for the *HSA*^{-/-}. A- T = 0, time of injury; B- T = 72h; C- T = 2 weeks. D. Table of the scoring results.

doi:10.1371/journal.pone.0139787.g003

Re-expression of *HSA* restored the healing phenotype

Next, we examined whether the expression of *HSA* in *HSA*^{-/-} mice restores the WT healing capabilities. Firstly, we verified that the viruses infected the cells *in vivo*. To that end, *in vivo* imaging of the wounded tissue in the WT mice 96hours after virus injection/dropping confirmed the expression of *mCherry* and *HSA* in the wounded tissue (Fig 6).

Then the importance of *HSA* in the healing process was evaluated by an additional experiment that was performed as described in Table 3. Briefly, mice from each genotype were randomly divided into groups of three mice. Longitudinal incisions of 1.5 cm were made on their back and the HIV-encoding viruses were administered by injection into the cells on the wound border or by dropping of the viruses into the wounded area. The healing was monitored every day for one week. Re-expression of *HSA* restores the healing phenotype in the *HSA*^{-/-} mice while the expression of the control *mCherry* vector had no effect (Fig 7).

Overexpression of *HSA* in WT mice improves wound healing

We further evaluated the ability of *HSA* to improve the wound healing process in normal *HSA*^{+/+} WT mice. For this purpose, we enlarged the wound size and the experiment was

Table 2.

	Grade 0	Grade 1	Grade 2	Grade 3
Collagen	Collagen arranged in tightly cohesive well demarcated bundles with a smooth dense bright homogeneous polarization pattern with normal crimping	Diminished fiber polarization: separation of individual fibers with maintenance of demarcated bundles	Bundle changes: separation of fibers with loss of demarcation of bundles giving rise to expansion of the tissue overall and clear loss of normal polarization pattern	Marked separation of fibers with complete loss of architecture
	Wt, KO = t = 0		Wt = 72h	KO = 72h

doi:10.1371/journal.pone.0139787.t002

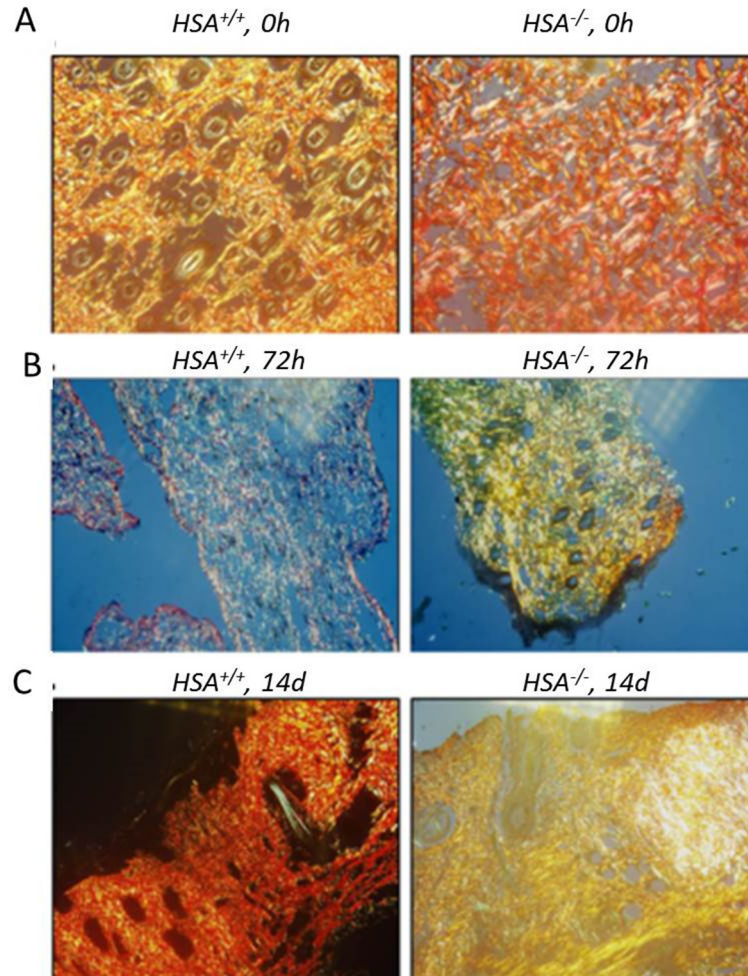


Fig 4. Collagen stains. Tissue sections were stained with NovaUltra™ Picro-Sirius Red stain and visualized on an Olympus AH light microscope at 400× magnification. The left picture in each panel represents the *HSA*^{+/+} mouse while the right is for the *HSA*^{-/-}. A. t = 0, time of injury, B. t = 72h, C. t = 14 days. The scoring is detailed in [Table 2](#).

doi:10.1371/journal.pone.0139787.g004

performed as described in [Table 4](#). Briefly, *HSA*^{+/+} mice were randomly divided into groups of four mice. Longitudinal incisions of 4-cm were made on their back and the mCherry or HSA-encoding viruses were administrated twice, 0 and 24 hours post-injury, by injection into the cells in the wound border or by dropping of the viruses into the wounded area and the healing rate was monitored. The results ([Fig 8](#)) suggest that overexpression of HSA resulted in faster and improved healing even in *HSA*-expressing mice. Already after 24 hours it was shown that there were differences in the healing rate between mice that were administrated with mCherry and HSA.

In order to confirm the importance of CD24/HSA in the healing process, a complementary experiment was performed. *HSA*^{+/+} mice were randomly divided into groups of three mice. Longitudinal incisions of 2 cm were made on their back and the anti-HSA M1/69 mAb (10 mg/kg) was administrated immediately post-injury by injection into the cells in the wound border. The results suggest that antibody-mediated reduction of HSA expression level caused to slower and non-homogenous healing in *HSA*-expressing mice ([Fig 9](#)).

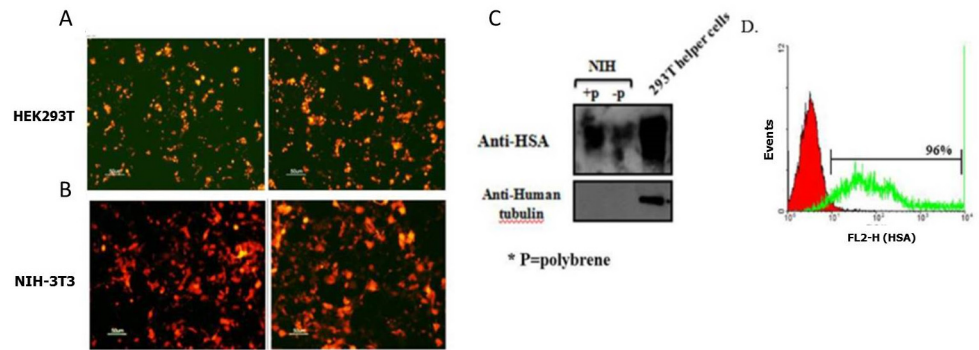


Fig 5. Production of HIV-based viruses for gene delivery. HEK 293T cells were co-transfected with the mentioned plasmids and after 48 h the expression of the transgene was evaluated by the mCherry marker (A). The infectivity of the virions, which was produced by the HEK293T helper cells, was tested on NIH-3T3 *in vitro* by fluorescence microscope (mCherry expression) (B). 72 h after the infection, cell lysates were prepared and 20 µg of total proteins was loaded. HSA was detected with the anti-HSA mAb, M1.69, and then the membrane was reprobed with anti-human tubulin (C). 1×10^6 infected cells were incubated with 10 µg/ml of M1.69 for 30 minutes at RT. FITC-labeled goat anti-rat antibody was used for the detection of bound antibody. The red curve represents the negative control (secondary antibody alone) and the green curve represents the binding of M1.69 (D).

doi:10.1371/journal.pone.0139787.g005

The improvement of healing by HSA expression does not depend on the mice strain

In order to examine if the above phenotype depends on the mice strain, we compared between Balb/C and C57Bl/6JWtmice. Eight mice from each strain were randomly divided to two groups of four mice. One group of each strain was injected with HSA-encoding viruses, immediately after the injury, while the second group with the control vector. According to our observations, the wound healing was improved regardless of the mice strain as can be demonstrated in Fig 10.

Discussion

Our study shows that HSA in mice plays an important role in wound healing. Restoration of the protein restores impaired wound healing back to normal. Moreover, forced expression of HSA enhances the healing process.

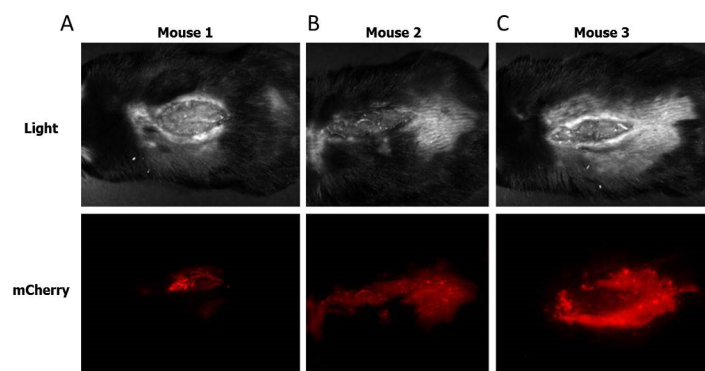


Fig 6. Imaging of the living organism. The viruses were injected or dropped into the wounded cells immediately after the injury, on $t = 0.96$ h after injection into the cells on the wound border (A) or dripping (B-C) of the mCherry-encoded viruses ($n = 3$) onto the wound area, mice were taken to *in vivo* imaging to detect the mCherry expression in the wounded cells using the Cri Maestro device. This imaging tool enables multiplexed *in vivo* fluorescence imaging of small animals with high sensitivity.

doi:10.1371/journal.pone.0139787.g006

Table 3.

	Number of mice	Mice genotype	Length of cut	
Group 1	3	<i>HSA</i> ^{+/+}	1.5 cm	Only wound
Group 2	3	<i>HSA</i> ^{+/+}	1.5 cm	HIV-mCherry injection
Group 3	3	<i>HSA</i> ^{+/+}	1.5 cm	HIV-mCherry dropping
Group 4	3	<i>HSA</i> ^{+/+}	1.5 cm	HIV-HSA injection
Group 5	3	<i>HSA</i> ^{+/+}	1.5 cm	HIV-HSA dropping
Group 6	3	<i>HSA</i> ^{-/-}	1.5 cm	Only wound
Group 7	3	<i>HSA</i> ^{-/-}	1.5 cm	HIV-mCherry injection
Group 8	3	<i>HSA</i> ^{-/-}	1.5 cm	HIV-mCherry dropping
Group 9	3	<i>HSA</i> ^{-/-}	1.5 cm	HIV-HSA injection
Group 10	3	<i>HSA</i> ^{-/-}	1.5 cm	HIV-HSA dropping

doi:10.1371/journal.pone.0139787.t003

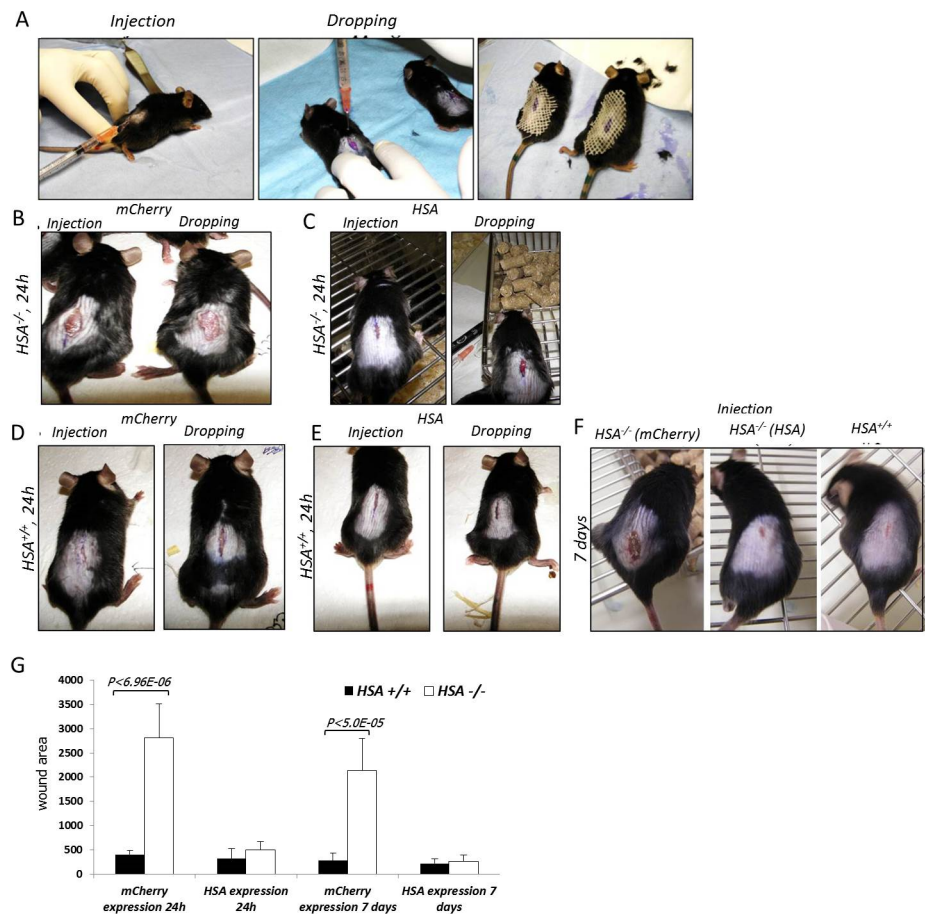


Fig 7. Re-expression of HSA. A-The viruses were injected or dropped into the wounded cells on T = 0; B- *HSA*^{-/-} mice 24 h after mCherry-encoded viruses injection (left panel) or dropping (right panel); C-*HSA*^{-/-} mice 24 h after HSA encoded viruses injection (left panel) or dropping (right panel); D-*HSA*^{+/+} mice 24 h after mCherry-encoded viruses injection (left panel) or dropping (right panel); E-*HSA*^{+/+} mice 24 h after mCherry-encoded viruses injection (left panel) or dropping (right panel); F- 7 days after viruses injection; G- A representative plot of the statistical differences, in size of wound area, between the groups.

doi:10.1371/journal.pone.0139787.g007

Table 4.

	Wound size	Treatment	Administration
Group 1	4 cm	NO	
Group 2	4 cm	mCherry (T = 0, 24h)	dropping
Group 3	4 cm	mCherry (T = 0, 24h)	Injection
Group 4	4 cm	HSA (T = 0, 24h)	dropping
Group 5	4 cm	HSA (T = 0, 24h)	Injection

doi:10.1371/journal.pone.0139787.t004

CD24 expression has long been correlated with pathologies associated with tumor cell migration and invasion [21–23]. The exact function and mechanism of action of CD24 is mostly unknown; however, it is thought to be involved in a variety of processes such as cell proliferation and it also changes the adhesive properties of tumor cells by promoting their adhesion to P-selectin, fibronectin, collagens I and IV, and laminin [22]. Tumors have been

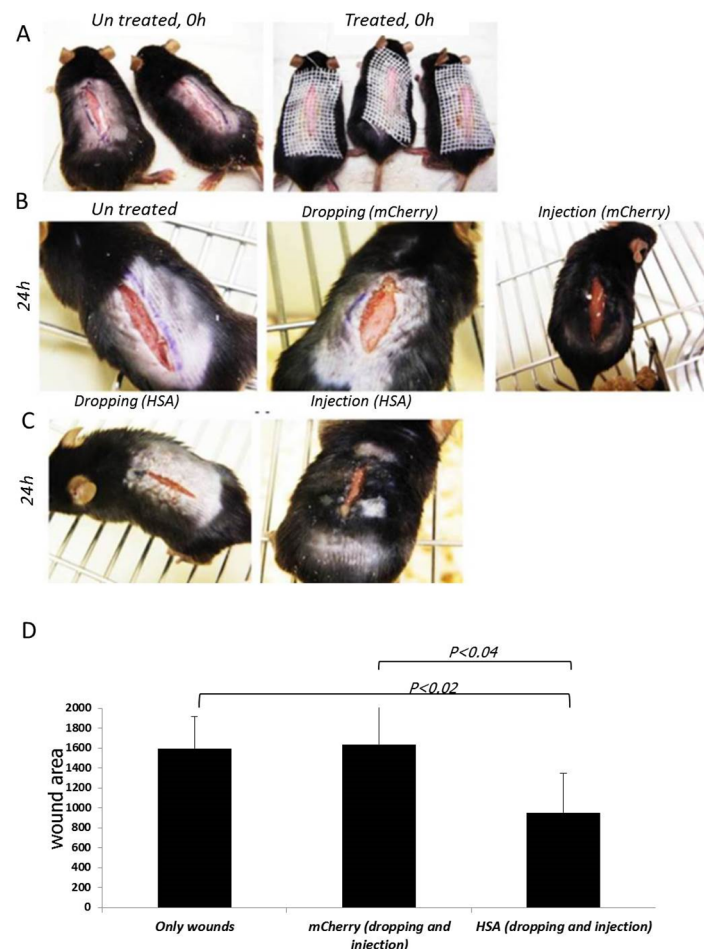


Fig 8. Acceleration of wound healing upon over expression of HSA. A-The wounds were infected with the viruses (right panel) or left un-treated (left panel) on T = 0; B- *HSA*^{+/+} mice 24 h after the injury (left panel), 24 h after infection, by dropping, with the mCherry-encoded viruses (middle panel), 24 h after mCherry-encoded viruses injection (right panel); C- *HSA*^{+/+} mice 24 h after infection, by dropping (left panel) or injection (right panel), with the HSA-encoded viruses; D- A representative plot of the statistical differences, in size of wound area, between the groups.

doi:10.1371/journal.pone.0139787.g008

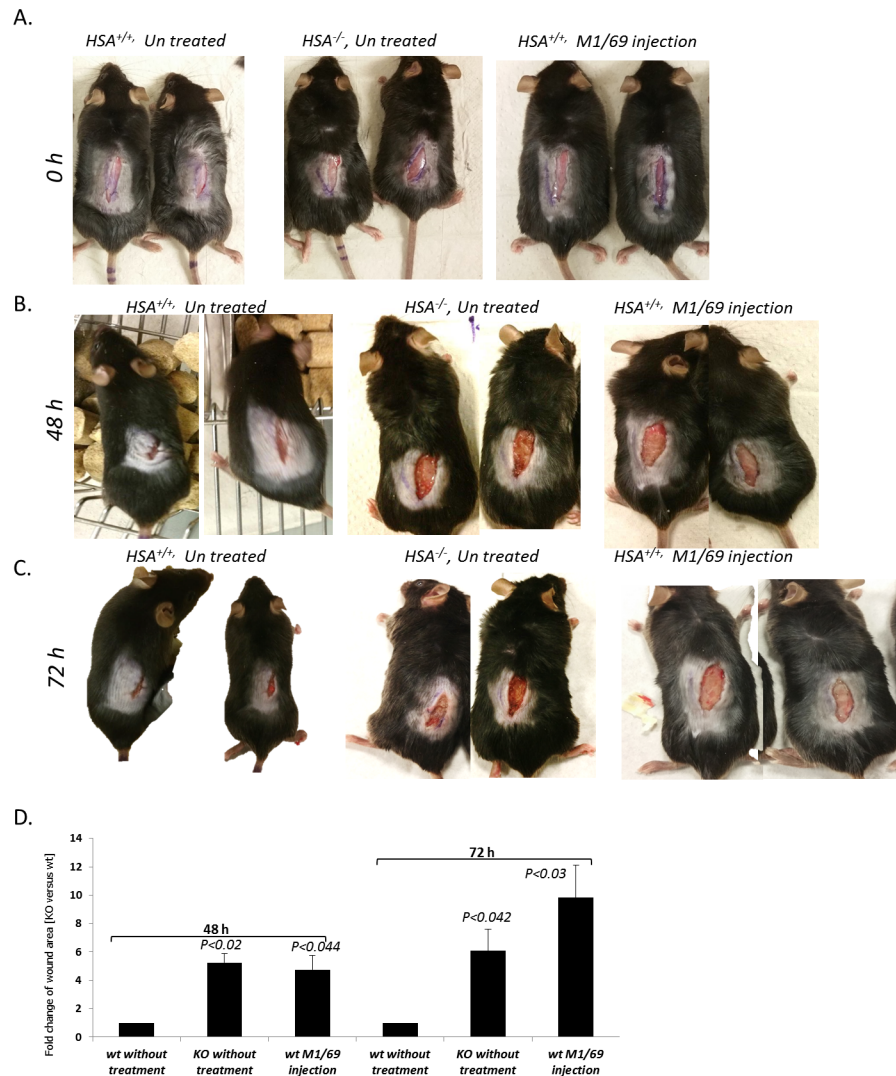


Fig 9. Delayed wound healing upon down regulation of HSA expression. A-The wounds were treated with anti-HSA antibody (right panel) or left un-treated (left and middle panel) on T = 0; B- *HSA*^{+/+} (left panel) and *HSA*^{-/-} (middle panel) mice 48 h after the injury and *HSA*^{+/+} mice 48 h after antibody injection (right panel); C- *HSA*^{+/+} (left panel) and *HSA*^{-/-} (middle panel) mice 72 h after the injury and *HSA*^{+/+} mice 72 h after antibody injection (right panel); D- A representative plot of the statistical differences, in size of wound area, between the groups. Student t-test was calculated in each time point between the tested group and the wt without treatment group.

doi:10.1371/journal.pone.0139787.g009

previously described as wounds that do not heal. Wound healing and cancer have similar properties of cellular behavior. They are both characterized by increased cell proliferation, survival, invasion and migration (e.g. angiogenesis and metastasis), remodeling of extracellular matrix, new blood vessel formation, and modulation of blood coagulation. The molecular programs in normal wound healing and those in tumor progression and metastasis were found to be similar [24,25], [26]. Data from our laboratory suggest that overexpression of CD24 is associated with increased cell migration in wound healing assays *in vitro* (Naumov et al., 2014)[27] showed that cells that overexpress CD24 proliferate faster, and increase cell motility, saturation density, plating efficiency, and growth in soft agar. They also produce larger tumors in nude mice as compared to the parental cells. In addition, We have shown, Shapira et al., JBC 2011,

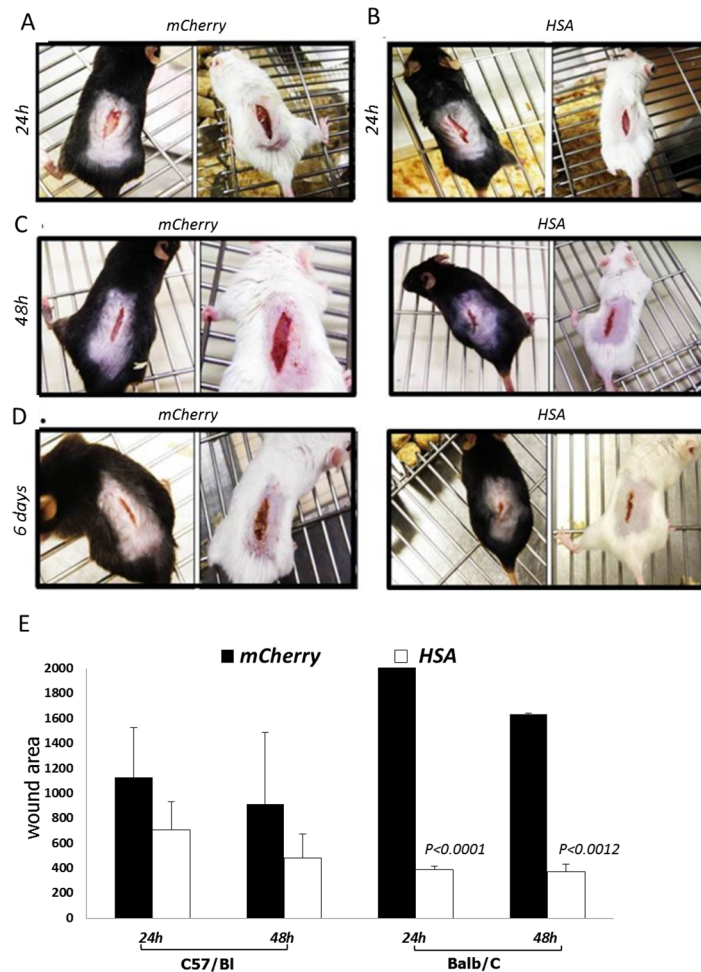


Fig 10. The rapid healing does not depend on mice strain. Four groups of four mice were used in this study. Two of them were of C57/Bl while the other two were of Balb/c. The mice in one group from each strain were injected with the HSA-encoded viruses while the other group with the mCherry-encoded viruses. A- *HSA*^{+/+} mice 24 h after mCherry-encoded viruses injection; B- *HSA*^{+/+} mice 24 h after HSA-encoded viruses injection; C- *HSA*^{+/+} mice 48 h after mCherry-encoded viruses (the two pictures on the left) and HSA-encoded viruses injection (the two pictures on the right); D- *HSA*^{+/+} mice 6 days after mCherry-encoded viruses (the two pictures on the left) and HSA-encoded viruses injection (the two pictures on the right); E-A representative plot of the statistical differences, in size of wound area, between the groups. Student t-test was calculated in each time point between the HSA treated group and the mCherry treated group.

doi:10.1371/journal.pone.0139787.g010

[28] that induced expression of CD24 in a dose- and time-dependent fashion (using the Tet-On system), led to an increased proliferation which was inhibited by mAb to CD24. *In vivo*, significantly larger tumors were developed in tetracycline-fed mice compared to the control group. Taking all of this together with the data presented here, we suggest that increased expression of CD24 promotes growth pathways and thus accelerates and improves the healing of wounded tissue. *HSA*-deficient mice have delayed healing. When the wounds were stitched, the stitches did not hold, suggesting that CD24 is required. In most cases, the healing process was not only delayed but it failed to progress through the normal stages of healing, and resulted in an inflamed scar. Most importantly, re-expression of HSA in *HSA*-deficient mice, by lentiviruses, restores the wound closure rate in WT mice.

Topical administration of anti-HSA antibodies confirms the genotypic observations of the importance of HSA in normal wound healing.

Interestingly, preliminary data emerging from mouse models of bone (tibia fracture model) fracture and tooth extraction strengthen the importance of CD24 in fracture and tooth extraction healing (Arber *et al.*, unpublished data).

Our hypothesis is that CD24 plays a key role in cell proliferation, migration and adhesion of healthy cells to the damaged area to restore normal tissue. Increased expression of the CD24 protein may represent a novel clinical intervention strategy to accelerate the healing of debilitating acute or chronic wounds in patients.

Acknowledgments

The authors are grateful to Esther Eshkol for meticulous editing of our paper.

Author Contributions

Conceived and designed the experiments: SS OBA NA JM EG. Performed the experiments: SS OBA. Analyzed the data: SS OS. Contributed reagents/materials/analysis tools: SS OBA DK OS. Wrote the paper: SS. Edited the paper: SK EG. Histology: OS.

References

1. Zcharia E, Zilka R, Yaar A, Yacoby-Zeevi O, Zetser A, et al. (2005) Heparanase accelerates wound angiogenesis and wound healing in mouse and rat models. *FASEB J* 19: 211–221. PMID: [15677344](#)
2. Tonnesen MG, Feng X, Clark RA (2000) Angiogenesis in wound healing. *J Invest Dermatol Symp Proc* 5: 40–46. PMID: [11147674](#)
3. Martin P (1997) Wound healing—aiming for perfect skin regeneration. *Science* 276: 75–81. PMID: [9082989](#)
4. Singer AJ, Clark RA (1999) Cutaneous wound healing. *N Engl J Med* 341: 738–746. PMID: [10471461](#)
5. Werner S, Grose R (2003) Regulation of wound healing by growth factors and cytokines. *Physiol Rev* 83: 835–870. PMID: [12843410](#)
6. Devalaraja RM, Nanney LB, Du J, Qian Q, Yu Y, et al. (2000) Delayed wound healing in CXCR2 knockout mice. *J Invest Dermatol* 115: 234–244. PMID: [10951241](#)
7. Martin P, Leibovich SJ (2005) Inflammatory cells during wound repair: the good, the bad and the ugly. *Trends Cell Biol* 15: 599–607. PMID: [16202600](#)
8. Jaakkola P, Kontusaari S, Kauppi T, Maata A, Jalkanen M (1998) Wound reepithelialization activates a growth factor-responsive enhancer in migrating keratinocytes. *FASEB J* 12: 959–969. PMID: [9707168](#)
9. Kristiansen G, Sammar M, Altevogt P (2004) Tumour biological aspects of CD24, a mucin-like adhesion molecule. *J Mol Histol* 35: 255–262. PMID: [15339045](#)
10. Suzuki T, Kiyokawa N, Taguchi T, Sekino T, Katagiri YU, et al. (2001) CD24 induces apoptosis in human B cells via the glycolipid-enriched membrane domains/rafts-mediated signaling system. *J Immunol* 166: 5567–5577. PMID: [11313396](#)
11. Kadmon G, von Bohlen und Halbach F, Schachner M, Altevogt P (1994) Differential, LFA-1-sensitive effects of antibodies to nectadrin, the heat-stable antigen, on B lymphoblast aggregation and signal transduction. *Biochem Biophys Res Commun* 198: 1209–1215. PMID: [8117278](#)
12. Aigner S, Ruppert M, Hubbe M, Sammar M, Sthoeger Z, et al. (1995) Heat stable antigen (mouse CD24) supports myeloid cell binding to endothelial and platelet P-selectin. *Int Immunol* 7: 1557–1565. PMID: [8562500](#)
13. Aigner S, Sthoeger ZM, Fogel M, Weber E, Zarn J, et al. (1997) CD24, a mucin-type glycoprotein, is a ligand for P-selectin on human tumor cells. *Blood* 89: 3385–3395. PMID: [9129046](#)
14. Aigner S, Ramos CL, Hafezi-Moghadam A, Lawrence MB, Friederichs J, et al. (1998) CD24 mediates rolling of breast carcinoma cells on P-selectin. *FASEB J* 12: 1241–1251. PMID: [9737727](#)
15. Ahmed MA, Jackson D, Seth R, Robins A, Lobo DN, et al. CD24 is upregulated in inflammatory bowel disease and stimulates cell motility and colony formation. *Inflamm Bowel Dis* 16: 795–803. doi: [10.1002/ibd.21134](#) PMID: [19998456](#)

16. Shapira S, Kazanov D, Weisblatt S, Starr A, Arber N, et al. The CD24 protein inducible expression system is an ideal tool to explore the potential of CD24 as an oncogene and a target for immunotherapy in vitro and in vivo. *J Biol Chem* 286: 40548–40555. doi: [10.1074/jbc.M111.286534](https://doi.org/10.1074/jbc.M111.286534) PMID: [21976680](https://pubmed.ncbi.nlm.nih.gov/21976680/)
17. Sagiv E, Memeo L, Karin A, Kazanov D, Jacob-Hirsch J, et al. (2006) CD24 is a new oncogene, early at the multistep process of colorectal cancer carcinogenesis. *Gastroenterology* 131: 630–639. PMID: [16890615](https://pubmed.ncbi.nlm.nih.gov/16890615/)
18. Wang W, Wang X, Peng L, Deng Q, Liang Y, et al. CD24-dependent MAPK pathway activation is required for colorectal cancer cell proliferation. *Cancer Sci* 101: 112–119. doi: [10.1111/j.1349-7006.2009.01370.x](https://doi.org/10.1111/j.1349-7006.2009.01370.x) PMID: [19860845](https://pubmed.ncbi.nlm.nih.gov/19860845/)
19. Jacobi J, Tam BY, Sundram U, von Degenfeld G, Blau HM, et al. (2004) Discordant effects of a soluble VEGF receptor on wound healing and angiogenesis. *Gene Ther* 11: 302–309. PMID: [14737090](https://pubmed.ncbi.nlm.nih.gov/14737090/)
20. Maffulli N, Longo UG, Franceschi F, Rabitti C, Denaro V (2008) Movin and Bonar scores assess the same characteristics of tendon histology. *Clin Orthop Relat Res* 466: 1605–1611. doi: [10.1007/s11999-008-0261-0](https://doi.org/10.1007/s11999-008-0261-0) PMID: [18437501](https://pubmed.ncbi.nlm.nih.gov/18437501/)
21. Bretz N, Noske A, Keller S, Erbe-Hofmann N, Schlange T, et al. CD24 promotes tumor cell invasion by suppressing tissue factor pathway inhibitor-2 (TFPI-2) in a c-Src-dependent fashion. *Clin Exp Metastasis* 29: 27–38. doi: [10.1007/s10585-011-9426-4](https://doi.org/10.1007/s10585-011-9426-4) PMID: [21984372](https://pubmed.ncbi.nlm.nih.gov/21984372/)
22. Baumann P, Cremers N, Kroese F, Orend G, Chiquet-Ehrismann R, et al. (2005) CD24 expression causes the acquisition of multiple cellular properties associated with tumor growth and metastasis. *Cancer Res* 65: 10783–10793. PMID: [16322224](https://pubmed.ncbi.nlm.nih.gov/16322224/)
23. Lim SC, Oh SH (2005) The role of CD24 in various human epithelial neoplasias. *Pathol Res Pract* 201: 479–486. PMID: [16164042](https://pubmed.ncbi.nlm.nih.gov/16164042/)
24. Hanahan D, Weinberg RA (2000) The hallmarks of cancer. *Cell* 100: 57–70. PMID: [10647931](https://pubmed.ncbi.nlm.nih.gov/10647931/)
25. Dauer DJ, Ferraro B, Song L, Yu B, Mora L, et al. (2005) Stat3 regulates genes common to both wound healing and cancer. *Oncogene* 24: 3397–3408. PMID: [15735721](https://pubmed.ncbi.nlm.nih.gov/15735721/)
26. Dvorak HF (1986) Tumors: wounds that do not heal. Similarities between tumor stroma generation and wound healing. *N Engl J Med* 315: 1650–1659. PMID: [3537791](https://pubmed.ncbi.nlm.nih.gov/3537791/)
27. Naumov I, Zilberberg A, Shapira S, Avivi D, Kazanov D, et al. (2014) CD24 knockout prevents colorectal cancer in chemically induced colon carcinogenesis and in APC(Min)/CD24 double knockout transgenic mice. *Int J Cancer* 135: 1048–1059. doi: [10.1002/ijc.28762](https://doi.org/10.1002/ijc.28762) PMID: [24500912](https://pubmed.ncbi.nlm.nih.gov/24500912/)
28. Shapira S, Kazanov D, Weisblatt S, Starr A, Arber N, et al. (2011) The CD24 protein inducible expression system is an ideal tool to explore the potential of CD24 as an oncogene and a target for immunotherapy in vitro and in vivo. *J Biol Chem* 286: 40548–40555. doi: [10.1074/jbc.M111.286534](https://doi.org/10.1074/jbc.M111.286534) PMID: [21976680](https://pubmed.ncbi.nlm.nih.gov/21976680/)